Predicting Mutual Entrainment of Oscillators with Experiment-Based Phase Models

István Z. Kiss, Yumei Zhai, and John L. Hudson*

Department of Chemical Engineering, 102 Engineers' Way, University of Virginia, Charlottesville, Virginia 22904-4741, USA

(Received 24 February 2005; published 20 June 2005)

We show that mutual entrainment in interacting oscillators can be characterized using phase models that are developed from direct experiments with a single oscillator. The models are used to predict order-disorder transitions in populations and the dependence of order on system parameters; the description is verified in independent experiments in sets of chemical oscillators. The experiment-based model properly describes in-phase and antiphase mutual entrainment with positive and negative interactions in small sets as well as dynamical clustering in populations of oscillators.

DOI: 10.1103/PhysRevLett.94.248301 PACS numbers: 82.40.Np, 05.45.Xt

The characterization of synchronization of oscillators, of importance in various physical [1], chemical [2], and biological [3] systems, can be a difficult and challenging task. Complexity arises at hierarchal levels; changes in parameters have effects on the characteristics of single oscillators and consequently alter collective behavior in nontrivial ways. A standard approach of system description, the development of a model of the individual units and their means of interaction, requires detailed knowledge of kinetic and transport processes. A complementary approach is the use of a phase model [3,4] in which each oscillator is represented by a single variable, its phase. A central element of such models is an interaction function that characterizes the extent of phase advance or delay as a result of interaction between two oscillators [4,5]. Theoretical studies and numerical simulations have shown that phase models can capture the important synchronization properties of populations with weak interactions [3,4,6–12].

In this Letter, we demonstrate the power of phase models, obtained solely from direct experiments on a single oscillator, in predicting the dependence of synchronization characteristics such as order-disorder transitions on system parameters in small sets and large populations of interacting oscillators. The interaction functions are obtained from experimental phase response curves. We investigate the parametric dependence of mutual entrainment using an electrochemical reaction system, the electrodissolution of nickel in sulfuric acid.

The experiments were carried out in a standard three electrode electrochemical cell containing 3 $\mathrm{mol/dm^3}$ sulfuric acid at 11 °C with a 1 mm diameter Ni working, a $Hg/Hg_2SO_4/K_2SO_4$ reference, and a Pt counter electrode [13]. The Ni electrode, connected to the potentiostat through a series resistor $R = 652\ \Omega$, was held at constant circuit potential V. Current $i(t)$ was measured at 250 Hz. Sets of two or 64 Ni electrodes were connected to the potentiostat through one series (collective) resistor, R_s, and through two (or 64) parallel resistors, R_p. The interaction strength $K = NR_s/R_p$ was controlled through the external resistors by keeping the equivalent (individual) resistance $R_{eq} = R_p + NR_s = 652\ \Omega$ constant. (N is the number of electrodes.)

Consider first a single oscillator. Two major characteristic waveforms of periodic oscillations are the smooth and relaxation types. In nickel electrodissolution both types can be seen. At low circuit potentials [Fig. 1(a)] the waveform is smooth (nearly sinusoidal with constant angular

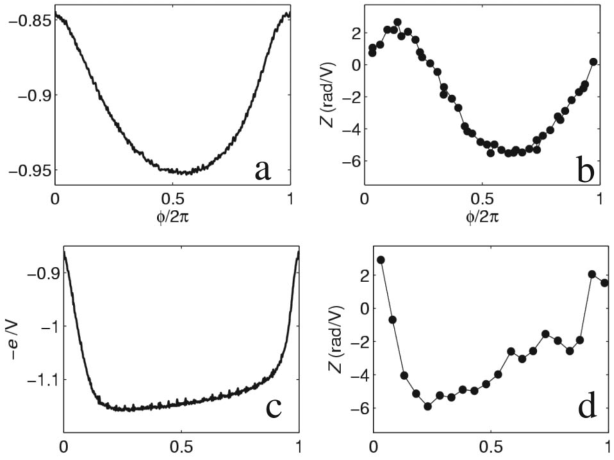

FIG. 1. Waveform and response function of the oscillations in metal dissolution experiments. (a) Electrode potential $e(t) = V - i(t)R$ as a function of phase $[\phi(t)]$ for a smooth oscillator; $\phi(t) = 2\pi t/T$, where $T = 2.26$ s is the period, t is the time from the maximum of the oscillation, and $V = 1.105$ V is the circuit potential. (b) Response function (or infinitesimal phase response curve) (Z) of a smooth oscillator at $V = 1.105$ V. The response function is obtained from the phase response curve ($\Delta\Phi$ vs ϕ). Phase advance ($\Delta\Phi$) of the oscillations due to a short (8 ms) perturbation of the circuit potential (with an amplitude of −300 mV, resulting in $\Delta e = 40$ mV change in electrode potential) as a function of phase was obtained. The phase advance was calculated from the inherent (free-running) period and the period observed during the perturbation cycle (T_{pert}): $\Delta\Phi = 2\pi(1 - T_{\text{pert}}/T)$. The response function is $Z(\phi) = \Delta\Phi(\phi)/\Delta e$. (c) Electrode potential as a function of phase for a relaxation oscillator ($V = 1.275$ V, $T = 2.77$ s). (d) Response function (Z) of a relaxation oscillator ($V = 1.275$ V).

velocity) whereas at large potentials [Fig. 1(c)] the oscillations have a relaxation character in which a fast linear deactivation is followed by a (initially slow) nearly exponential increase. The circuit potential thus can be used to tune the relaxation character of the oscillations in this chemical reaction system.

The response function $Z(\phi)$ [4,7] shows the phase advance per unit perturbation as a function of the phase of the oscillator. The response function is proportional to the phase response curve widely used in circadian rhythms [5] to interpret external entrainment. As expected for a simple smooth oscillator, the phase response curve in Fig. 1(b) has a nearly sinusoidal shape. For the relaxation oscillator the phase response curve [Fig. 1(d)] is more asymmetric; in the linear deactivation region the system is quite unresponsive (with smaller values of phase advance or delay); the system is more responsive in the beginning of the excitatory state.

We obtain an experimental interaction function from the response function for use in the phase model description:

$$\frac{d\phi_i}{dt} = \omega_i + \sum_{j=1}^{N} H(\phi_j - \phi_i), \tag{1}$$

where ϕ_i and ω_i are the phase and frequency, respectively, of the ith oscillator and $H(\Delta\phi)$ is the interaction function that depends on the phase difference $\Delta\phi = \phi_j - \phi_i$ between two oscillators. Equation (1) shows that the phase of an oscillatory system increases at a rate equal to its inherent frequency slightly modified by slowing down or speeding up due to interactions with the other elements. The interaction function can be calculated from the phase response curve obtained with the variable through which the oscillators are coupled [4,7]; here the electrode potential

$$H(\Delta\phi) = \frac{1}{2\pi}\int_{\phi=0}^{2\pi} Z(\phi)K[e_j(\phi + \Delta\phi) - e_i(\phi)]d\phi, \tag{2}$$

where $e_j(\phi)$ and $e_i(\phi)$ are the waveforms of oscillators i and j (here they are assumed to be identical), and K is the interaction strength of linear difference coupling. The interaction function at various phase differences is shown in the left panel of Fig. 2(a) for the smooth oscillator; the shape consists of $[1 - \cos\Delta\phi]$ and $\sin\Delta\phi$ components characteristic of those found for an oscillator close to a supercritical Hopf bifurcation [4]. The values of H are zero at $\Delta\phi = 0$ and 2π as a result of the diffusive nature of the coupling. For most of the phase difference, H is positive implying [from Eq. (1)] that the oscillators have a tendency to speed up as a result of the coupling.

An important quantity for synchronization, the odd (antisymmetric) part of the interaction function $H_-(\Delta\phi) = [H(\Delta\phi) - H(-\Delta\phi)]/2$, is shown in the right panel of Fig. 2(a). In a set of two coupled oscillators mutual entrainment occurs at phase difference $\Delta\phi^*$ given by $\Delta\omega/2 = H_-(\Delta\phi^*)$, where $\Delta\omega = \omega_2 - \omega_1$ is the frequency difference of the oscillators. Mutual entrainment of two identical oscillators with the interaction function of Fig. 2(a) will occur at $\Delta\phi^* = 0$ and π. Only the first of these is stable; a positive slope of the odd part of the interaction function at $\Delta\phi^*$ implies stable and a negative slope unstable entrainment [2,6]. Therefore, a set of two oscillators with the interaction function shown in Fig. 2(a) will be mutually entrained in an in-phase configuration (with a phase difference close to zero).

The interaction function for the relaxation oscillator [Fig. 1(c)] seen at a higher potential is shown in Fig. 2(c). Compared to the smooth case [Fig. 2(a)] the interaction function is more deformed with the maximum shifted to larger $\Delta\phi$ values. More pronounced changes occur in the odd part of the interaction function which is now a negative sine function with higher harmonic com-

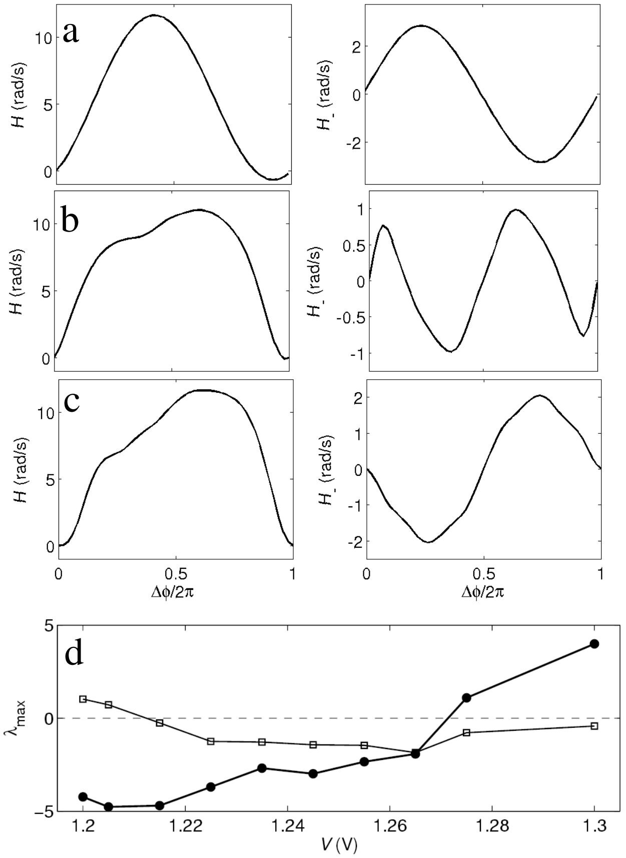

FIG. 2. Experimental interaction function and its prediction of mutual entrainment. (a)–(c) Interaction function $H(\Delta\phi)$ (left panel) and its odd part (right panel) at $V = 1.105$ V (smooth oscillator), 1.245, and 1.275 V (relaxation oscillator), respectively. ($K = 1.$) (d) Stability of the balanced clusters ($\lambda_{\max}$) as a function of the circuit potential. Solid circle: one-cluster. Open square: two-cluster. $\lambda_{\max}$ is the largest (nonzero) value of eigenvalues λ_p of the cluster solutions of Eq. (1). The eigenvalues of a balanced M cluster state of a system of N globally coupled oscillators with interaction function $H(\Delta\phi)$ are obtained [2,9] as: for $p = 0, 1, \ldots, M-1$: $\lambda_p = 1/M\Sigma_{k=0}^{M-1}F'(2\pi k/M)\times[1 - \exp(-2\pi ikp/M)]$; for $p = M, M+1, \ldots, N-1$: $\lambda_M = 1/M\Sigma_{k=0}^{M-1}F'(2\pi k/M)$. $F(\Delta\phi) = H(-\Delta\phi)$.

ponents. The change of the sign of the slope of the function at zero intersections implies that stable mutual entrainment would occur in an antiphase configuration at a phase difference $\Delta\phi^* = \pi$. This counterintuitive phenomenon, relevant in neuron dynamics [14], is called dephasing [10].

The transition from smooth $[H_-(\Delta\phi) \approx \sin(\Delta\phi)]$ to relaxation oscillations as the circuit potential is changed takes place with the addition of strong higher harmonic components. The odd part of the interaction function of a weakly relaxational oscillator [at a circuit potential between those of the smooth and the relaxational regions, Fig. 2(b)] is approximately $H_-(\Delta\phi) \approx \sin(2\Delta\phi)$. Both in-phase ($\Delta\phi^* = 0$) and antiphase ($\Delta\phi^* = \pi$) mutual entrainment states are stable; the attained state will depend on initial conditions.

The interaction functions shown in Fig. 2 were calculated with positive (excitatory) coupling. With negative (inhibitory) coupling there is a stability switch of the entrained states; smooth oscillators prefer antiphase and relaxation oscillators in-phase entrainment. The in- and antiphase synchronization of relaxation oscillators due to inhibitory and excitatory interactions has been a well-studied paradox of neuroscience; it has been suggested that a phase model description can be a useful tool for interpreting the synchronization [15–17].

The experimentally determined interaction functions can also be used to predict synchronization [4,5,11,12] and clustering [2,8,9,18] in populations of identical and nonidentical oscillators. (Clusters are groups of synchronized oscillators.) The stability of the balanced clusters obtained from the interaction function [2,9] as a function of the circuit potential is summarized in Fig. 2(d) (calculated with positive coupling). At lower circuit potentials where the individual oscillation is smooth only the one-cluster (fully synchronized) state is stable ($\lambda_{\max}$ is negative). As the potential increases the interaction function changes and the one-cluster state becomes unstable for $V \geq 1.275$ V. The two-cluster state, stable for $V \geq 1.215$ V, is the typical behavior of a relaxation oscillator. For $1.215\ \mathrm{V} \leq V \leq 1.265$ V, which lies between the smooth and highly relaxational regions, a bistability is predicted where both one- and two-cluster states are possible ($\lambda_{\max} < 0$). (At higher potentials stable three and four clusters are predicted due to the strong higher harmonic components of the interaction function.)

The above predictions on mutual entrainment, using a phase model obtained from experiments with a single oscillator, are now tested in experiments with two and 64 globally coupled oscillators. Without added coupling the oscillators are not synchronized and each has its own free-running period. Positive coupling of two smooth oscillators results in in-phase entrainment [Fig. 3(a)] and negative coupling yields nearly antiphase entrainment [Fig. 3(b)]; on the other hand, highly relaxation oscillators produce antiphase [Fig. 3(c)] and in-phase oscillations [Fig. 3(d)] with positive and negative coupling, respectively. Of particular note is the nearly identical synchronization that is seen with the negative coupling. The effect of the negative coupling is to increase differences in the potentials of the coupled oscillators; nevertheless, the oscillators synchronize at almost zero phase difference as correctly predicted by the phase model. In the study of the population of 64 chemical oscillators, smooth oscillators synchronize in a single cluster and relaxational oscillators in a two-cluster state [13]. Experiments in a parameter region ($V = 1.265$ V) between these states, in which bistability is predicted, are shown in Fig. 3(e). A perturbation of the stable one-cluster state [left panel of Fig. 3(e)] yields a stable two-cluster state [right panel of Fig. 3(e)]. (A stable three-

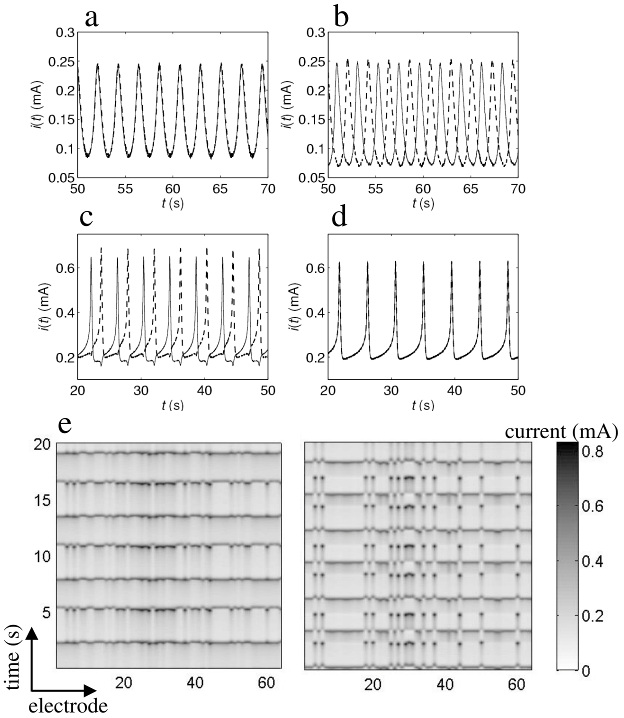

FIG. 3. Mutual entrainment of smooth and relaxation oscillators with positive (excitatory) and negative (inhibitory) coupling in experiments. (a) In-phase entrainment of two smooth oscillators with positive coupling. $K = 0.25$ (K is the strength of electrical coupling), $V = 1.105$ V. Without coupling the frequencies of the oscillators are $\omega_1 = 0.471$ Hz and $\omega_2 = 0.466$ Hz. (b) Antiphase entrainment of smooth oscillators with negative coupling. $K = -0.26$, $V = 1.105$ V. [Negative coupling was achieved with a negative differential resistance ($R_s < 0$) feedback circuit built in the potentiostat.] (c) Antiphase entrainment of two relaxation oscillators with positive coupling. $K = 0.30$, $V = 1.300$ V. $\omega_1 = 0.157$ Hz, $\omega_2 = 0.198$ Hz. (A 30 Ω additional resistance was added to the electrode with longer period; this additional resistance decreases the period disparity between the oscillators.) (d) In-phase entrainment of two relaxation oscillators with negative coupling. $K = -0.32$, $V = 1.300$ V. (e) Stable one-cluster (left panel) and two-cluster (right panel) state of a population of globally coupled oscillators under the same experimental condition. $K = 1.5$, $V = 1.265$ V. The two-cluster state was obtained from the one-cluster state by a perturbation of the circuit potential at $\phi = 0.5$. (Amplitude: -600 mV, length: 250 ms.)

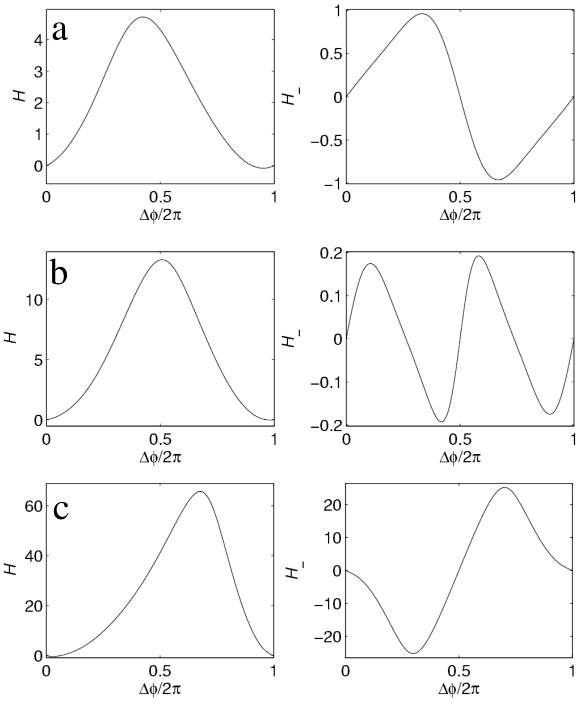

FIG. 4. Numerical simulations: interaction functions obtained with an ODE model. (a)–(c) Interaction function (left panel) and its odd part (right panel) at $V = 15$ (smooth oscillator), 24.77, and 26.3 (relaxation oscillator), respectively. The interaction function for the model was calculated with the software XPPAUT [21].

cluster was obtained at higher potential.) All the synchronization behavior seen in the experiments with both two and 64 oscillators are in agreement with the predictions of the interaction functions obtained from experiments on a single oscillator.

The interaction function is not constructed from ordinary differential equations (ODEs) describing material and charge balances but rather is obtained directly from the experimental phase response curves. For the chemical reaction system being treated here, however, there does exist a two-variable ordinary differential equation model [19] that captures the main dynamical features of the system and which can be used as a comparison of the phase model approach to the traditional approach using ODE models to characterize synchronization. Interaction functions obtained from the ODE model [20] for three representative potentials are shown in Fig. 4. As in the experimentally determined interaction functions shown in Fig. 2, the interaction function has predominantly positive values; with an increase of relaxation character the odd part changes from a nearly sine wave [smooth, Fig. 4(a)] through a $\sin(2\Delta\phi)$ [moderately relaxational, Fig. 4(b)] to an inverted sine wave with higher harmonics [strongly relaxational, Fig. 4(c)]. The ODE model captures the qualitative features of the synchronization during the transition from smooth to relaxation oscillators. Even in this relatively well-understood system, however, the phase model is superior in two respects in that not only does it not require detailed information on reaction kinetics and transport properties, but it also reproduces the transitions quantitatively. Therefore, the phase model approach can have application in systems in which a quantitative description is required but where kinetic information is difficult to obtain. Our findings show that phase models, derived with the assumption of weak coupling, hold in physically important ranges of interaction strengths that lead to mutual entrainment.

The method demonstrated here has application to various fields. In neural systems experiment-based phase models could help determine the importance of intrinsic cell properties on synchronization leading to essential or pathological rhythmic behavior [15,16].

Financial support from the National Science Foundation (CTS-0317762) is acknowledged. We thank Alexander Mikhailov and Hiroshi Kori for discussions.

---

*Electronic address: hudson@virginia.edu

[1] A. S. Pikovsky, M. Rosenblum, and J. Kurths, *Synchronization: A Universal Concept in Nonlinear Science* (Cambridge University Press, Cambridge, England, 2001).

[2] S. C. Manrubia, A. S. Mikhailov, and D. H. Zanette, *Emergence of Dynamical Order: Synchronization Phenomena in Complex Systems* (World Scientific, Singapore, 2004).

[3] A. T. Winfree, J. Theor. Biol. **16**, 15 (1967).

[4] Y. Kuramoto, *Chemical Oscillations, Waves and Turbulence* (Springer, New York, 1984).

[5] A. T. Winfree, *The Geometry of Biological Time* (Springer-Verlag, Berlin, 1980).

[6] H. Sakaguchi, S. Shinomoto, and Y. Kuramoto, Prog. Theor. Phys. **77**, 1005 (1987).

[7] G. B. Ermentrout and N. Kopell, J. Math. Biol. **29**, 195 (1991).

[8] D. Hansel, G. Mato, and C. Meunier, Phys. Rev. E **48**, 3470 (1993).

[9] K. Okuda, Physica D (Amsterdam) **63**, 424 (1993).

[10] S. K. Han, C. Kurrer, and Y. Kuramoto, Phys. Rev. Lett. **75**, 3190 (1995).

[11] H. Daido, Physica D (Amsterdam) **91**, 24 (1996).

[12] S. H. Strogatz, Physica D (Amsterdam) **143**, 1 (2000).

[13] I. Z. Kiss, W. Wang, and J. L. Hudson, J. Phys. Chem. B **103**, 11433 (1999).

[14] A. Sherman and J. Rinzel, Proc. Natl. Acad. Sci. U.S.A. **89**, 2471 (1992).

[15] B. Pfeuty *et al.*, J. Neurosci. **23**, 6280 (2003).

[16] G. B. Ermentrout and D. Kleinfeld, Neuron **29**, 33 (2001).

[17] D. Hansel, G. Mato, and C. Meunier, Europhys. Lett. **23**, 367 (1993).

[18] H. Kori, Phys. Rev. E **68**, 021919 (2003).

[19] D. Haim *et al.*, J. Phys. Chem. **96**, 2676 (1992).

[20] The ODE model is given in Ref. [13] ($R = 20$).

[21] B. Ermentrout, *Simulating, Analyzing, and Animating Dynamical Systems: A Guide to* XPPAUT *for Researchers and Students* (SIAM, Philadelphia, 2002).